Two-Stage Distributionally Robust Optimization for Energy Hub Systems

Pengfei Zhao, *Student Member, IEEE*, Chenghong Gu, *Member, IEEE*, Da Huo, Yichen Shen, and Ignacio Hernando-Gil, *Member, IEEE*

***Abstract*—Energy hub system (EHS) incorporating multiple energy carriers, storage and renewables can efficiently coordinate various energy resources to optimally satisfy energy demand. However, the intermittency of renewable generation poses great challenges on optimal EHS operation.**

This paper proposes an innovative distributionally robust optimization model to operate EHS with an energy storage system (ESS), considering the multimodal forecast errors of photovoltaic (PV) power. Both battery and heat storage are utilized to smooth PV output fluctuation and improve the energy efficiency of EHS. This paper proposes a novel multimodal ambiguity set to capture the stochastic characteristics of PV multimodality. A two-stage scheme is adopted, where i) the first stage optimizes EHS operation cost, and ii) the second stage implements real-time dispatch after the realization of PV output uncertainty. The aim is to overcome the conservatism of multimodal distribution uncertainties modelled by typical ambiguity sets and reduce the operation cost of EHS. The presented model is reformulated as a tractable semidefinite programming problem and solved by a constraint generation algorithm. Its performance is extensively compared with widely used normal and unimodal ambiguity sets. The results from this paper justify the effectiveness and performance of the proposed method compared to conventional models, which can help EHS operators to economically consume energy and use ESS wisely through the optimal coordination of multi-energy carriers.

***Index Terms*—Constraint generation algorithm, distributionally robust optimization, energy hub system, multimodal ambiguity set, renewable energy.**

NOMENCLATURE

A. Sets

T	Set of time periods.

B. Parameters

η_e, η_{th}	Electric and thermal efficiency of CHP.
η_f, η_{re}	Efficiency of GF and solar power.
COP	Coefficient of performance.
$\overline{P_{g,CHP}}, \overline{P_{e,HP}}, \overline{P_{g,GF}}$	Maximum input limit of CHP, GSHP and GF.
$\underline{P_{g,CHP}}, \underline{P_{e,HP}}$ $\underline{P_{g,GF}}$	Minimum input limit of CHP, GSHP and GF.
$\overline{P_{hs}^{ch}}$, $\underline{P_{hs}^{ch}}$	Maximum and minimum limit of charging power of heat storage.
$\overline{P_{hs}^{dch}}$, $\underline{P_{hs}^{dch}}$	Maximum and minimum limit of discharging power of heat storage.
$P_{hs}^{stb}(t)$	Standby power loss of heat storage at time t.
$E_{hs,min}, E_{hs,max}$	Minimum and maximum energy for heat storage.
$\eta_{hs}^{ch}, \eta_{hs}^{dch}$	Charging and discharging efficiency of heat storage.
$\overline{P_b^{ch}}$, $\underline{P_b^{ch}}$	Maximum and minimum limit of charging power of battery.
$\overline{P_b^{dch}}$, $\underline{P_b^{dch}}$	Maximum and minimum limit of discharging power of battery.
$E_{b,min}, E_{b,max}$	Minimum and maximum energy for battery.
$\eta_b^{ch}, \eta_b^{dch}$	Charging and discharging efficiency of battery.
$\omega_f(t)$	PV generation forecast at time t.
$\overline{P_{ele}}$, $\underline{P_{ele}}$	Maximum and minimum limit of electricity purchase.
$\overline{P_{gas}}$, $\underline{P_{gas}}$	Maximum and minimum limit of gas purchase.
$\pi_{ele}(t), \pi_{gas}(t)$	Electricity and gas purchase cost at time t.
$L_e(t), L_{th}(t)$	Electricity and heating demand at time t.
$\pi_s^r(t)$	Regulation cost coefficient of solar generation.

C. First-stage variables

$P_{g,CHP}(t)$, $P_{e,HP}(t)$,$P_{g,GF}(t)$	Input power of CHP, GSHP and GF.
$P_{hs}^{ch}(t)$, $P_{hs}^{dch}(t)$	Charging and discharging power of heat storage at time t.
$u_{hs}^{ch}(t)$, $u_{hs}^{dch}(t)$	Charging and discharging status of heat storage at time t.
$P_b^{ch}(t)$, $P_b^{dch}(t)$	Charging and discharging power of battery at time t.
$u_b^{ch}(t)$, $u_b^{dch}(t)$	Charging and discharging status of battery at time t.
$\omega_s(t)$	Scheduled PV generation at time t.
$P_{ele}(t)$	Electricity purchase at time t.
$P_{gas}(t)$	Gas purchase at time t.

Manuscript received July 8, 2019; revised August 13, 2019; accepted August 25, 2019.

P. Zhao, C.Gu (corresponding author) and Y. Shen are with the Department of Electronic & Electrical Engineering, University of Bath, Bath, UK.(e-mail: P. Zhao@bath.ac.uk; C.Gu@bath.ac.uk; Y.Shen@bath.ac.uk;).

D. Huo is with the School of Engineering, Newcastle University, UK. (e-mail:Da.Huo@newcastle.ac.uk).

I. Hernando-Gil is with the ESTIA Institute of Technology, France. (e-mail:I.Hernandogil@estia.fr).

$v_e(t)$, $v_g(t)$	Dispatch factors of electricity and gas
x	Vector of first-stage variables.

D. Second-stage variables

$\omega_r(t)$	Regulated PV generation at time t.
$P^r_{ele}(t)$	Regulated electricity purchase at time t.
$P^r_{gas}(t)$	Regulated gas purchase at time t.
y	Vector of second-stage variables.

E. Uncertainty

$\xi_s(t)$	Uncertainty of solar generation forecast.
μ_s, Σ_s	Mean vector and covariance matrix of ξ_s.
$D^T_{\xi_s}$, $D^M_{\xi_s}$, $D^U_{\xi_s}$	Ambiguity sets for ξ_s.
Ξ	Support of ξ_s.
Θ	Second moment matrix.
VS	Polyhedral set of extreme points.

I. Introduction

THE interdependencies between various energy carriers improve the flexibility and efficiency of power systems. As an interface between energy producers and consumers, energy hub systems (EHS) play a noteworthy role in integrating multiple carriers and generation resources to efficiently satisfy energy load [1]. In reality, shopping malls, industrial parks, university campus and hospitals can be modelled as EHS. For example, the EHS for Beijing's new subsidiary administrative center is proposed in [2], which supplies residential, commercial and administrative buildings. A residential EHS in Ontario, Canada is proposed in [3] for energy savings while maintaining the comfort level of household owners.

Energy storage systems (ESS) play a vital role in EHS due to the advantages of saving costs and smoothing renewable energy fluctuations [4]. Accordingly, to optimally coordinate various energy systems and ESS components in EHS, optimal operation has been modelled and resolved by many optimization techniques. The optimal dispatch of EHS is first investigated by using combined optimal power flow in [1]. An autonomous energy management of residential EHSs is proposed, considering each EHS as a self-interested agent [5], formulated as a monotone generalized Nash game. In [6] a combined method of energy loop intelligent searching, real nodes arrangement and virtual nodes insertion method is introduced to divide the complex EHS into several EHSs.

However, the uncertainty from the fluctuations in renewable generation and variations of load, leads to challenges in EHS economic operation. Among all proposed methods, stochastic optimization (SO) [4, 7, 8] and robust optimization (RO) [9, 10] are frequently used. Paper [11] proposes a hybrid scenario-based method to manage a distribution network connected EHS, which applies interval optimization and information gap decision theory. In [8], a stochastic dynamic optimization is used to minimize the functional risk of EHS operation cost. To enhance the computational reliability, a two-stage robust EHS at an integrated transmission and distribution level is proposed in [9]. Moreover, a tri-level RO is proposed in [10] for a coordinated regional-district EHS operation, which enhances system resilience against natural disasters while ensuring the economic operation.

In terms of uncertainty modelling, SO either relies on a vast number of samples to approximate distributions or fits data into empirical distributions, which could be overly optimistic. RO also considers the worst case via uncertainty sets, potentially resulting in over-conservative solutions. By contrast, distributionally robust optimization (DRO) avoids assuming a specific uncertainty distribution and yields less-conservative results. DRO has simpler requirements of uncertainties and is mathematically tractable, which accommodates distributions via an ambiguity set [12]. Additionally, DRO performs better in making the best use of limited statistical data and produces less-conservative results by considering the worst expectation over all possible distributions, compared to the traditional worst-case oriented RO. However, DRO has only been applied in investigating EHS planning in [13]. Other DRO related papers focus on unit commitment, economic dispatch, home energy management and regulation service in power markets.

A two-stage DRO for unit commitment considering wind uncertainty is proposed in [14]. Paper [15] proposes a two-stage security-constrained economic dispatch via DRO in a multi-period model. For consuming energy wisely by energy customers, a DRO based chance-constrained programming is proposed in [16] considering uncertainty from renewable resources. A two-stage stochastic program is used to model uncertainties in parameters of distributed energy resources and regulation signals where DRO based chance-constrained programming is applied in the second stage in [17]. The historical market data is used to learn the uncertainty distributions, which approximates the hourly average regulation signal to Gaussian distribution and accordingly an efficient second order cone programming model (SOCP) is obtained. However, this method is only limited to distributions which are similar to the empirical distributions, and thus cannot be applied to all the distributions, particularly multimodal distributions. If the multimodal distribution is approximated to empirical distributions, the original multimodality is ignored, leading to over-conservative solutions.

In the aforementioned literature, commonly used ambiguity sets are applied to fit all possible distributions without considering modality information, which only contain moment information of uncertain variables (referred as T-ambiguity set in this paper). However, the distributions of renewable forecast errors (e.g., solar forecast error) practically contain multi modes, and hence T-ambiguity set might cause unnecessary conservatism. Fig. 1 shows the histogram of a multimodal solar error forecast [18]. Paper [19] proves that ignoring the multimodality leads to over conservatism, thus resulting in prohibitively high costs. Multimodality can be incorporated into DRO to mitigate the conservatism because distributional information is further specified.

This paper designs a novel two-stage distributionally robust energy hub dispatch (DR-EHD) model, which incorporates photovoltaic (PV) arrays, energy converters, and an ESS. The EHS investigated represents a community-level building such

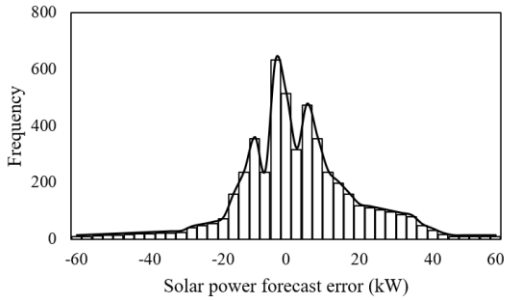

Fig. 1. Histogram of solar power forecast error.

as a hospital, shown in Fig. 2. A multimodal ambiguity set (M-ambiguity set) is developed, considering the conditional moment information of PV to characterize its multimodal distribution. The paper innovatively models the irregular solar power generation with multimodal distribution of forecast errors, characterized by an M-ambiguity set. The optimization objective is to minimize the expected operation cost by optimally scheduling energy hub resources over the operation horizon. The first stage determines the initial operation plan before the realization of solar power availability and the second stage minimizes the expectation of operation costs. The performance of using M-ambiguity set is extensively investigated and compared with using T-ambiguity set and a unimodal ambiguity set (U-ambiguity set) to highlight the advantage of the mitigated conservatism in M-ambiguity set.

The main contributions of this paper are as follows:

(1) For the first time in literature, it proposes a novel two-stage DRO to optimize energy hub operation and reduce the overly-conservatism of traditional RO [9], producing more cost-efficient operational strategies;

(2) Compared with papers [4, 7, 8], the proposed DR-EHD is less data-dependent by using moment and modality information of distributions, avoiding requiring extensive PV data that can break the privacy of local community energy usage.

(3) It develops two novel ambiguity sets: M-ambiguity set and U-ambiguity set to simulate the multimodal distributions of solar forecast errors, which can produce less-conservative results compared to commonly used T-ambiguity set [20, 21];

(4) The optimal EHS operation with multiple energy infrastructures under solar power output uncertainty is extensively investigated in the case study, which convincingly demonstrates that the M-ambiguity set can better characterize multimodal distributions, producing more accurate results.

The rest of this paper is organized as follows. Section II introduces the necessity of considering multimodal distributions. Section III proposes mathematical modelling for EHS. Section IV presents ambiguity sets for DRO. The methodology and solution algorithm are given in Section V. Section VI demonstrates case studies and performance of the DR-EHD. Conclusions are drawn in Section VII.

II. MULTIMODALITY IN PV OUTPUT DISTRIBUTIONS

Renewable generation data processing and forecasting always neglect small modes, assuming a large mode distribution with many small modes as unimodal distributions. For computation simplicity and efficiency, the data samples are normally approximated to empirical distributions, for example, solar [18, 22, 23] and wind output [24, 25] distributions.

However, it has been proved that the approximation of unimodal distribution could significantly deviate from actual scenarios, thus affecting the effectiveness of developed models and methods [18, 25]. By contrast, recorded data obtained from the National Data Buoy Center presents the multimodal distribution data of solar and wind output [18, 25]. Therefore, it is strongly necessary to model PV output by using multimodal distributions rather than unimodal distributions.

RO and SO, as two popular approaches to cope with the uncertainties of renewable generation, require uncertainty bounds and a large number of uncertain data samples. Thus, modality information is not required for RO and such information is already included in the distribution for SO. However, DRO, as it only requires partial distributional information, modality information is important for it. When more distributional information is considered, RO is closer to SO, improving mathematical performance.

It is noted that in previous DRO studies, only mean, variance and covariance are widely considered, which ignores other distributional information such as modality, skewness and kurtosis [11-13, 17]. The reason is that more distributional information brings a trade-off between objective conservatism and tractability, particularly for high dimensional mathematical problems. Recent literature [26-28] has proved that with the additional inclusion of distributional information in ambiguity sets, the objective costs can be reduced and reasonable computational tractability can be guaranteed. This paper considers multimodality for PV output, which is proved to be less conservative and tractable by semidefinite programming (SDP) reformulation.

III. DISTRIBUTIONALLY ROBUST OPTIMIZATION

The theory of DRO is introduced in this section. A brief introduction of DRO approach is proposed, followed by the description of three types of ambiguity sets.

A. Introduction of DRO

Compared with RO, which additionally considers the stochastic nature of uncertain parameters, DRO is developed to address the conservatism of RO. Ambiguity set is used to accommodate all the possible distributions of uncertain parameters, which has the same statistical information. The distributional uncertainty has been expressed and specified by various ambiguity sets [12, 29], mostly using the moment information. The ambiguity set with the first and second moments are proved to be efficiently tractable and have been applied widely in power systems [14, 15, 21, 30]. However, some solar power forecast error distributions are obtained as multimodal [18, 22, 23] and ambiguity sets disregarding the multimodality will produce overly conservative results [19].

B. Proposed Ambiguity Sets

In this paper, The M-ambiguity set $D_{\xi_s}^{M}$ is mainly discussed and other two ambiguity sets are constructed for comparison. The three ambiguity sets $D_{\xi_s}^{T}$, $D_{\xi_s}^{M}$ and $D_{\xi_s}^{U}$ are presented in (1)-(3) respectively, which are described as follows:

T-ambiguity set $D_{\xi_s}^{T}$: Using a large ambiguity set, e.g., T-ambiguity set, to accommodate a large range of distributions

can ensure the true uncertainty distribution. Equation (1) ensures that the integral of probability ξ_s is 1 while the true mean μ_{s1} and covariance Σ_{s1} are known. However, if ambiguity set is too large, this will prevent the optimization from searching for the real structure of the true distribution. With multimodality specified, M-ambiguity set is smaller and expected to have better performance.

M-ambiguity set $D_{\xi_s}^{M}$: Because the multimodal forecast error distribution is considered in this paper, the ambiguity set is built incorporating two uncertain variables ξ_s and $\tilde{s}$. In equation (2), it is based on the work proposed in [19], where distribution P incorporates *m* distinct distributions $\mathrm{P}_1,\ldots,\mathrm{P}_m$. $\tilde{s}$ is introduced to model the non-negligible effect on ξ_s, which represents modality information that could affect the distribution of ξ_s. Accordingly, based on $\tilde{s}$, conditional mean vector μ_{s2} and covariance matrix Σ_{s2} with known mode positions are used to construct the M-ambiguity set $D_{\xi_s}^{M}$. The sample data is strictly restricted within a bound in each $\tilde{s}$, in case of overlapping with other $\tilde{s}$.

U-ambiguity set $D_{\xi_s}^{U}$: To test the assumption that multimodal distribution contains only the largest mode without other small modes, $D_{\xi_s}^{U}$ is established to model the multimodal distribution by a representative unimodal distribution. Equation (3) ensures that the integral of probability ξ_s is 1 while the true mean μ_{s3} and covariance Σ_{s3} are known. According to [26], an unimodal probability distribution P_α is defined as the distribution with the requirement of α-unimodality, where α is the degree of unimodality. When $\alpha = 1$, the distribution peaks only at the mode and is non-increasing away from the mode, which is a classical unimodality problem. It should be noted that the M-ambiguity set also needs to ensure α-unimodality of each mode. For fixed modes in this paper, a constraint needs to be added as in (4), where $m_s$is the location of modes.

The ambiguity sets are proposed as follows, where $(\cdot)'$ represents the transposition of $(\cdot)$.

$$D_{\xi_s}^{T} = \left\{ f(\xi_s) \left| \begin{array}{c} \mathrm{P}\{\xi_s\} = 1 \\ \mathrm{E}\{\xi_s\} = \mu_{s1} \\ \mathrm{E}\{\xi_s(\xi_s)'\} = \Sigma_{s1} + \mu_{s1}(\mu_{s1})' \end{array} \right. \right\} \tag{1}$$

$$D_{\xi_s}^{M} = \left\{ f(\xi_s) \left| \begin{array}{c} (\xi_s, \tilde{s}) \sim \mathrm{P}_\alpha \\ \mathrm{P}_\alpha\{\xi_s|\tilde{s}\} = 1 \\ \mathrm{E}_\alpha\{\xi_s|\tilde{s}\} = \mu_{s2} \\ \mathrm{E}_\alpha\{\xi_s(\xi_s)'|\tilde{s}\} = \Sigma_{s2} + \mu_{s2}(\mu_{s2})' \end{array} \right. \right\} \tag{2}$$

$$D_{\xi_s}^{U} = \left\{ f(\xi_s) \left| \begin{array}{c} \mathrm{P}_\alpha\{\xi_s\} = 1 \\ \mathrm{E}_\alpha\{\xi_s\} = \mu_{s3} \\ \mathrm{E}_\alpha\{\xi_s(\xi_s)'\} = \Sigma_{s3} + \mu_{s3}(\mu_{s3})' \end{array} \right. \right\} \tag{3}$$

$$\left(\frac{\alpha+2}{\alpha}\right)(\Sigma_s - \mu_s(\mu_s)') \succ \frac{1}{\alpha^2}(\mu_s - m_s)(\mu_s - m_s)' \tag{4}$$

IV. Energy Hub System Modelling

The configuration and mathematical modelling of EHS are illustrated in this section. The EHS includes PV arrays, ESS, combined heat and power (CHP), gas furnace (GF), and ground source heat pump (GSHP). The purpose of this paper is to demonstrate the multimodal uncertainty handled by the novel ambiguity set and solved by DRO approach. It is noted that there are many uncertainties in EHS operation, such as PV generation, load and energy price. This paper will only focus on the uncertainty of PV generation, but the developed model is applicable to other uncertainties with multimodal distributions.

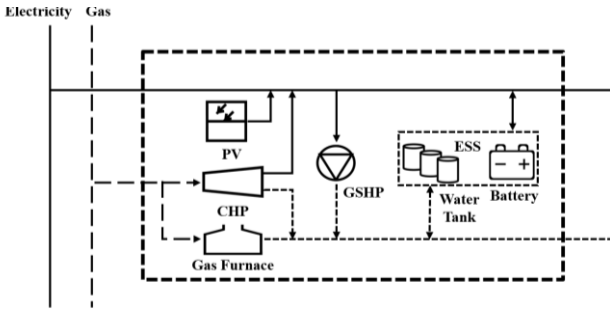

Fig. 2. Overview schematic of EHS.

A. EHS Configuration

An EHS achieves the functions of generation, conversion, storage and consumption of multiple energy carriers. The EHS is supplied by electricity and gas purchased from the upstream energy grids. Solar power is directly harnessed by PV with associated converters to supply electrical load. The ESS is used to store excessive electricity and heat.

B. Mathematical Formulation of EHS Components

1) Energy Converters

Multiple energy converters are applied to collectively utilize gas and electricity: CHP generates electricity and heat simultaneously via consuming natural gas, GF combusts gas to produce heat, and electricity is converted to heat by GSHP to extract heat from the ground to satisfy heating load. The relationship between the inputs and outputs of all energy converters are described from (5) to (8). The input power for each energy converter is constrained in (9) to (11).

$$P_{CHP,Eout}(t) = \eta_e P_{g,CHP}(t)\ ,\ \forall t \in T \tag{5}$$

$$P_{CHP,Hout}(t) = \eta_{th} P_{g,CHP}(t)\ ,\ \forall t \in T \tag{6}$$

$$P_{HP,out}(t) = COP\ P_{e,HP}(t)\ ,\ \forall t \in T \tag{7}$$

$$P_{GF,out}(t) = \eta_f P_{g,GF}(t)\ ,\ \forall t \in T \tag{8}$$

$$\underline{P_{g,CHP}} \le P_{g,CHP}(t) \le \overline{P_{g,CHP}}\ ,\ \forall t \in T \tag{9}$$

$$\underline{P_{e,HP}} \le P_{e,HP}(t) \le \overline{P_{e,HP}}\ ,\ \forall t \in T \tag{10}$$

$$\underline{P_{g,GF}} \le P_{g,GF}(t) \le \overline{P_{g,GF}}\ ,\ \forall t \in T \tag{11}$$

2) Energy Storage System

The ESS consists of both heat and electricity storage. As for the heat storage system, water tank is used for space heating which can supply heating load, such as residential heat, ventilation and air conditioning (HVAC). For simplicity, the subscript $\{\cdot\}$ is used to represent the index $\{hs, b\}$. The excessive heat can be stored in the water tank for later consumption. Status variables, $u_{hs}^{ch}(t)$, $u_{hs}^{dch}(t)$ u_b^{ch} and u_b^{dch}, are used to control its charging and discharging in (14). Equations (12) and (13) limit the amounts of charging and discharging heat and power. The remaining power and hear are defined in (15), where the water tank standby loss is also

defined. The remaining thermal and power energy within the heat and electricity storage are constrained by (16).

$$u^{ch}_{\{\cdot\}}(t)\underline{P^{ch}_{\{\cdot\}}} \le P^{ch}_{\{\cdot\}}(t) \le u^{ch}_{\{\cdot\}}(t)\overline{P^{ch}_{\{\cdot\}}}, \forall t \in T \quad (12)$$

$$u^{dch}_{\{\cdot\}}(t)\underline{P^{dch}_{\{\cdot\}}} \le P^{dch}_{\{\cdot\}}(t) \le u^{dch}_{\{\cdot\}}(t)\overline{P^{dch}_{\{\cdot\}}}, \forall t \in T \quad (13)$$

$$u^{ch}_{\{\cdot\}}(t) + u^{dch}_{\{\cdot\}}(t) \le 1, \forall t \in T \quad (14)$$

$$E_{\{\cdot\}}(t) = E_{\{\cdot\}}(t-1) + \sum_1^t P^{ch}_{\{\cdot\}}(t)\eta^{ch}_{\{\cdot\}} - P^{dch}_{\{\cdot\}}(t)/\eta^{dch}_{\{\cdot\}} + P^{stb}_{\{\cdot\}}(t), \ \forall t \in 2 \ldots T \quad (15)$$

$$E_{\{\cdot\},min} \le E_{\{\cdot\}}(t) \le E_{\{\cdot\},max}, \forall t \in T \quad (16)$$

3) Solar Power Generation

In the first stage, (17) ensures the scheduled PV generation not to exceed the forecast values and in the second stage, the regulated solar generation in (18) is constrained by the new availability considering the uncertainty of forecasting error. It is noted that among all error distributions of solar power forecasting, there are inevitably multimodal distributions [18]. This work is to handle such multimodal distributions of solar forecast errors, which are shown in Fig. 1.

$$0 \le \omega_s(t) \le \omega_f(t) \quad (17)$$

$$0 \le \omega_r(t) \le \omega_f(t) + \xi_s(t) \quad (18)$$

4) Energy Purchase from Upstream Energy Grids

For expression simplicity, the subscript $\{\cdot\}$ is used to represent the index $\{ele, gas\}$. Electricity and gas purchases are constrained in (19), where the costs are shown in (20), in terms of the unit cost of energy purchase, i.e., $\pi_{\{\cdot\}}(t)$. The energy purchase in the second stage are constrained by (21).

$$\underline{P_{\{\cdot\}}} \le P_{\{\cdot\}}(t) \le \overline{P_{\{\cdot\}}} \quad (19)$$

$$EC_{\{\cdot\}} = \pi_{\{\cdot\}}(t)\, P_{\{\cdot\}}(t), \forall t \in T \quad (20)$$

$$\underline{P_{\{\cdot\}}} \le P^r_{\{\cdot\}}(t) \le \overline{P_{\{\cdot\}}} \quad (21)$$

5) Coupling Relationship

In Fig. 2, the demand, including electricity $L_{ele}(t)$ and heat$L_{th}(t)$, is satisfied by electricity and gas purchase $P_{ele}(t)$ and $P_{gas}(t)$, solar power generation and ESS supply. The coupling between demand and energy supply is shown in (22), where $v_e(t)$ represents the electricity injection to GSHP and $v_g(t)$ indicates the proportion of gas injection to CHP.

$$\begin{bmatrix} L_{ele}(t) + P_b(t) \\ L_{th}(t) + \tau_h(t) \end{bmatrix} = \begin{bmatrix} 1 - v_e(t) & \eta_{re}(1 - v_e(t)) & v_g(t)\eta_e(1 - v_e(t)) \\ v_e(t)COP & v_e(t)\eta_{re}COP & v_g(t)(\eta_{th} + \eta_e v_e(t)COP + \eta_f - v_g(t)\eta_f) \end{bmatrix} \times \begin{bmatrix} P_{ele}(t) \\ \omega_{s/r}(t) \\ P_{gas}(t) \end{bmatrix} \quad (22)$$

C. DR-EHD Objective Function

The objective function of the two-stage DR-EHD is to minimize the operation cost, presented as follows:

$$\min \sum_{t\in T} EC_{ele} + EC_{gas} + \sup_{P\in D^T_{\xi_s}, D^M_{\xi_s}, D^U_{\xi_s}} E_P[Q(x,\xi_s)], \quad \forall t \in T \quad (23)$$

s.t. (5)-(22)

$$Q(x,\xi_s) = \sum_{t\in T} \pi^r_s(t)\,|\omega_r(t) - \omega_s(t)| + \pi^r_{ele}(t)|P^r_{ele}(t) - P_{ele}(t)| + \pi^r_{gas}(t)\left|P^r_{gas}(t) - P_{gas}(t)\right|, \forall t \in T \quad (24)$$

Where $Q(x,\xi_s)$ represents the optimal regulation cost of solar power and energy purchase, which is a function of x, y and ξ_s. Here the regulation cost results from the difference between the scheduled and regulated power. The objective function in (22) contains: 1) the initial plan at the first stage to determine the energy purchase based on the forecast PV generation and 2) recourse actions of resources when the uncertainty of solar power is realized. The EHS operator determines the worst expected cost at the second stage by updating decisions on the energy purchase with the full uncertainty information.

V. Methodology

This section contains the solution procedure of the DR-EHD problem. The objective and constraints are all modelled in the compact form. Then, the dual formulation of the second-stage problem is formulated, followed by an SDP reformulation of the master problem. Finally, the constraint generation algorithm (CGA) is used to solve DR-EHD.

A. Abstract Formulation

The compact forms of (23) and (24) are in (25) and (27) respectively for clarity and simplicity in DR-EHD.

$$\min_{x\in X} c'x + \sup_{P\in D_{\xi_s}} E_P[Q(x,\xi_s)] \quad (25)$$

$$\text{s.t. } Ax \le b, \quad (26)$$

$$Q(x,\xi_s) = \min_y f'y \quad (27)$$

$$\text{s.t. } Ex + Fy + G\xi_s \le h, \quad (28)$$

Where, (28) represents constraints (18), (20)-(22), vector f corresponds to the coefficients of (24) and y is the second-stage decision variables.

B. Dual Form of the Second-stage Objective Function

The probability densities in (1)-(3) are variables to be optimized and thus the optimization problem contains a finite number of constraints and an infinite number of variables. To make the problem tractable, the primal problem is transformed into the dual form, which contains a finite number of variables.

S(x) is the objective function of the second-stage problem, $\sup_{P\in D^T_{\xi_s}, D^M_{\xi_s}, D^U_{\xi_s}} E_P[Q(x,\xi_s)]$ in an explicit primal form. ψ_0, ψ_j and Ψ_{jk} are the dual variables associated with constraints (31) to (33). $P(\xi_s)$ is the probability density function.

$$S(x)^{primal} = \max_{P(\xi_s)\in D_{\xi_s}} \int_\Xi Q(x,\xi_s)\, P(\xi_s) d\xi_s \quad (29)$$

$$\text{s.t. } P(\xi_s) \ge 0, \forall \xi_s \in \Xi \quad (30)$$

$$\int_\Xi P(\xi_s) d\xi_s = 1 \quad (31)$$

$$\int_\Xi \xi_s^j P(\xi_s) d\xi_s = \mu_j, j=1,2, \ldots, \Xi \quad (32)$$

$$\int_\Xi \xi_s^j \xi_s^k P(\xi_s) d\xi_s = \Sigma_{jk} + \mu_j\mu_k, j, k=1, \ldots, \Xi \quad (33)$$

According to the dual theory [12], the dual form of (29) is described as (34). Thus, the results of (34) are equal to those of

(29) when the covariance matrix is strictly positive [29, 31]. In (29), $P(\xi_s)$ is the decision variable and the problem (29)-(33) has an infinite number of variables and a finite number of constraints. After dual formulation, the problem (34)-(35) has a finite of variables and an infinite number of constraints, which is easier to solve.

$$S(x)^{dual} = \min_{\Psi,\psi,\psi_0} \langle \Psi'\Theta \rangle + \psi'\mu + \psi_0 \tag{34}$$

$$\text{s.t. } (\xi_s)'\Psi\xi_s + \psi'\xi_s + \psi_0 \geq Q(x,\xi_s) \quad \forall \xi_s \in \Xi \tag{35}$$

Where Θ denotes $\Sigma + \mu_s(\mu_s)'$, and $\langle A \rangle$ is the trace of matrix A.

Thus, the compact form of DR-EHD is

$$\min_{x\in X} c'x + S(x)^{dual} \tag{36}$$

C. SDP Reformulation

The proposed DR-EHD can be formulated as an SDP problem, thus to be tractable. The new dual variable τ is introduced to represent the dual form of (27). Accordingly, (27) and (28) can be represented in the following closed form [32]:

$$\max_{u\in ES} \tau'(b - Ex - G\xi_s) \tag{37}$$

$$VS = \{\tau | F'\tau = f, \tau \leq 0\} \tag{38}$$

Thus, constraint (35) can be expressed in the closed form, where VS is the polyhedral set of extreme points. Based on the new dual variable, (35) can be rewritten as (39). Note that this explicit expression (39) is a positive quadratic function of ξ_s.

$$(\xi_s)'\Psi\xi_s + (\psi + G'\tau^i)'\xi_s + \psi_0 - (h - Ex)\tau^i \geq 0 \quad \forall \xi_s \in \Xi,\ i = 1,2,\ldots,N_v \tag{39}$$

Where N_v is the cardinality of vertices of VS. Finally, the two-stage DR-EHD can be written in the following SDP model.

$$\min_{x,\Psi,\psi,\psi_0} c'x + \langle \Psi'\Theta \rangle + \psi'\mu + \psi_0 \tag{40}$$

$$\text{s.t. } \begin{bmatrix} \Psi & \frac{1}{2}(\psi + G'\tau^i) \\ \frac{1}{2}(\psi + G'\tau^i)' & \psi_0 - (h - Ex)'\tau^i \end{bmatrix} \geq 0 \quad i = 1,2,\ldots,N_v, \forall \tau^i \in VS, x \in X$$

D. Constraint Generation Algorithm

Although the original problem is transformed into a reformulated SDP, there are still a vast number of constraints in (40) within the VS, causing it challenging to solve. The reason is that the cardinality of VS is extremely large. The practical strategy is to only consider a part of vertices in a relaxed SDP problem for optimal solutions and the rest of the vertices can be relaxed temporarily. New vertices are then iteratively added until the optimal solutions are found. CGA can be summarized in the flowchart Fig. 3. CGA iteratively solves the master and sub problems by initializing a subset of all vertices and then gradually enlarges the set until the optimal solution is obtained.

The master and sub problems are described in (40) and (41):

$$(\xi_s)'\Psi\xi_s + \psi'\xi_s + \psi_0 - (h - Ex - G\xi_s)'\tau \geq 0 \quad \text{s.t. } \forall \xi_s \in \Xi, \tau \in VS \tag{41}$$

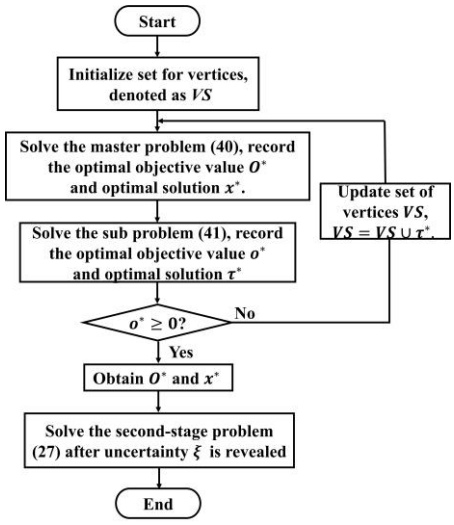

Fig. 3. Flowchart of constrained generation algorithm.

E. Overall Implementation

The methodology to solve the two-stage EHS operation is summarized by the following steps:

Step 1. Obtain data of electric and heating load of EHS, mean and covariance matrix of solar forecast error, time-varying energy price, and system parameters.

Step 2. Build the optimization model with constraints and objectives in both first and second stages.

Step 3. Establish the ambiguity sets $D_{\xi_s}^T$, $D_{\xi_s}^M$ and $D_{\xi_s}^U$ for solar forecast error.

Step 4. Set up the abstract formulation for the objective function and constraints.

Step 5. Introduce the dual variables and convert the problem into dual formulations.

Step 6. Reformulate the original problem into SDP and solve it by CGA.

VI. Case Studies

This section demonstrates the results of the proposed EHS. Firstly, the DR-EHD method derived by utilizing M-ambiguity set is presented. Secondly, the comparison among the use of three ambiguity sets is illustrated in terms of operation costs. Thirdly, the Skewness is analyzed to demonstrate the impact of moving locations of modes on optimization results. The comparison between RO and DRO has been thoroughly investigated in [15, 21]. Load profiles, hourly electricity price in upstream energy grids, and other system parameters given in Table I are taken from [4, 33]. A fixed gas tariff of 0.018 $/kWh is considered during the entire scheduling horizon. The

TABLE I
Parameters of DR-EHS

System parameters	
CHP	η_e=0.33, η_{th}=0.57, $\overline{P_{g,CHP}}$=600, $\underline{P_{g,CHP}}$=0
GSHP	COP=3, $\overline{P_{e,HP}}$=900, $\underline{P_{e,HP}}$=0
GF	η_f=0.7, $\overline{P_{g,GF}}$=900, $\underline{P_{g,GF}}$=0
Water tank	$0 \leq E_{hs}(t) \leq$ 100kWh, η_{hs}^{ch}= 0.85, η_{hs}^{dch}= 0.85
Battery	$0 \leq E_b(t) \leq$ 200kWh, η_b^{ch}= 0.88, η_b^{dch}= 0.88
Energy purchase	$0 \leq P_{ele}(t) \leq$ 500kW, $0 \leq P_{gas}(t) \leq$ 2000kW

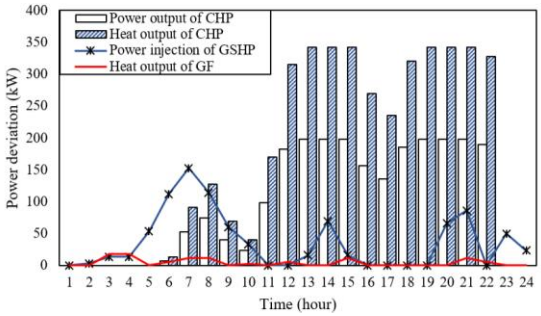

Fig. 4. Converter scheduling result in EHS.

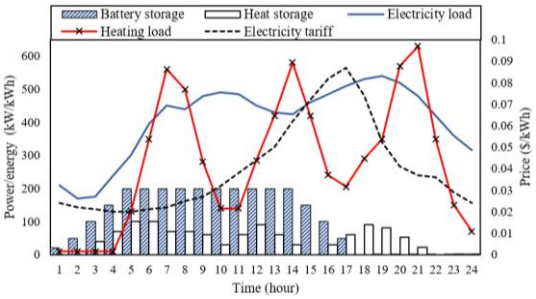

Fig. 5. Remaining energy of ESS.

electrical and heating load profiles are shown in Fig. 5.

A. *The Optimal Strategy for DR-EHD*

The optimal scheduling of energy converters over 24 hours based on DRO with M-ambiguity set is depicted in Fig. 4. As seen, GF is rarely used over the whole-time horizon due to lower efficiency compared with other energy converters. The maximum heat output of GF over the day is only 10 kW. GSHP intensively works between 3:00 and 10:00, 13:00 and 15:00, 20:00 and 24:00. It is injected by 545 kWh heat in the morning and peaks at 134kW, producing 1635 kWh heat. This large amount of heat can be stored by the water tank for later use. Comparatively, CHP is extensively utilized, especially between 11:00 and 22:00. Its output peaks at 342kW and heat output peaks at 198kW. The total heat conversion is 82% higher than the total electricity conversion. Possible reasons are: 1) Heat converters are directly connected to external gas purchase while electricity is directly consumed without conversion; 2) The gas injection to the CHP is converted to both power and heat with each corresponding efficiency. Because of the higher heat transferring efficiency, the heat output of CHP yields 24 % more than electricity generation.

To study the effectiveness of optimal ESS scheduling by DR-EHD, Fig. 5 depicts the remaining energy of ESS at each hour. The battery charges from 1:00 to 5:00 when the electricity price is relatively low. Between 5:00 and 14:00, it maintains a full charging state since electrical load is still low, and it is more economical to purchase energy from the grid. From 14:00 to 17:00, the battery discharges with increasing demand. Due to the limited capacity of battery, the excessive PV energy is not absorbed by the battery, but it is converted through the efficient GSHP and stored as heat energy by the heat storage system. The three heating load peaks result in the discharge of heat storage during 6:00-10:00, 12:00-15:00 and 19:00-22:00.

B. *Comparison of Ambiguity Sets*

The three ambiguity sets $D_{\xi_s}^T$, $D_{\xi_s}^M$ and $D_{\xi_s}^U$ are extensively compared in this section in terms of a) first-stage cost, b) average second-stage cost, c) average total cost, d) scheduled electricity purchase and e) scheduled gas purchase. From the results in Table II under three different ambiguity sets, it can be seen that the use of $D_{\xi_s}^T$ results in the highest results, followed by $D_{\xi_s}^U$, and $D_{\xi_s}^M$ yields the lowest results.

TABLE II
RESULTS OF THREE DIFFERENT AMBIGUITY SETS

	$D_{\xi_s}^T$	$D_{\xi_s}^M$	$D_{\xi_s}^U$
First-stage cost ($)	441.4	365.5	375.3
Average second-stage cost ($)	14.9	11.6	12.8
Average total cost ($)	456.3	377.1	388.1
Scheduled electricity purchase (kWh)	8228.5	7621.2	7836.6
Scheduled gas purchase ($)	7192.9	6980.5	7012.2

The average total cost by using $D_{\xi_s}^T$ is 456.3$, as compared to 377.1$ with $D_{\xi_s}^M$ is. By this comparison, it can be found that the conservatism can be reduced when the additional distribution characteristics is specified in the ambiguity set. It proves that $D_{\xi_s}^M$, with multiple means and covariance information, behaves less conservative than $D_{\xi_s}^T$ with only one aggregated mean and covariance information.

The reason to apply the $D_{\xi_s}^U$ is that some distributions contain a large mode and several small modes, where the small modes are ignored here for simplicity. The total cost from using $D_{\xi_s}^U$ is 388.1$, which is 83% and 103% of the result obtained from using $D_{\xi_s}^T$ and $D_{\xi_s}^M$ (456.3$ and 377.1$). Although results from using $D_{\xi_s}^U$ are lower than using $D_{\xi_s}^T$, which is less conservative, but technically, it is not accurate to model the multimodal distribution with $D_{\xi_s}^U$. This paper assumes the largest mode to be the representative mode where $m_s = 0$ but ignores other modes, based on the limited historical distribution.

Variability of the uncertain solar forecast error influences the optimization performance. Adding a risk measure can help to avoid extreme error data, in effect avoiding poor DR-EHD performance. The average total cost with different variances is shown in Fig. 6. It is found that with the increase of the variance, all the results are gradually increasing. As expected, the result by using T-ambiguity set is the highest, around 460$. Average costs by using M-ambiguity set is the lowest, fluctuating around 380$.

To further present the advantage of M-ambiguity set, KL-divergence as a widely-used measure to quantify the statistical distance between two distributions [34], is used here to change the size of the ambiguity set. In this paper, it is noted that the KL-divergence is not contained in the ambiguity sets but used to simply alter the size by controlling the number of possible distributions. The histogram in Fig. 1 is the empirical reference distribution. The distance between the considered distribution and reference distribution is defined as $\overline{d_{KL}} = d_{KL}/d_{KL,max}$, which varies between 0 and 1. As observed from Fig. 7, changing distance impacts both the expected total cost and variance. The performance of $D_{\xi_s}^M$ outperforms $D_{\xi_s}^T$ and $D_{\xi_s}^U$ for the entire range of distances. The average total cost decreases with increasing distance until $\overline{d_{KL}} = 0.1$, which then increases afterwards.

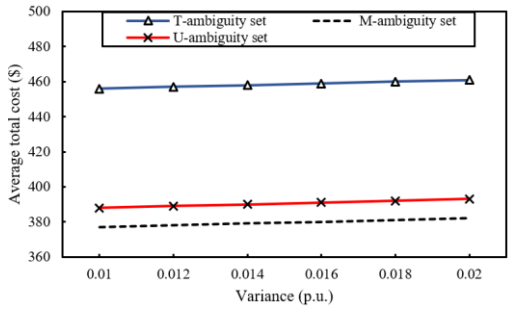

Fig. 6. Average total cost with three ambiguity sets in different variances.

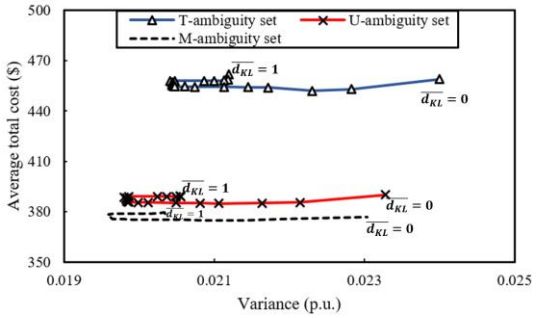

Fig. 7. Average total cost with three ambiguity sets in different sizes.

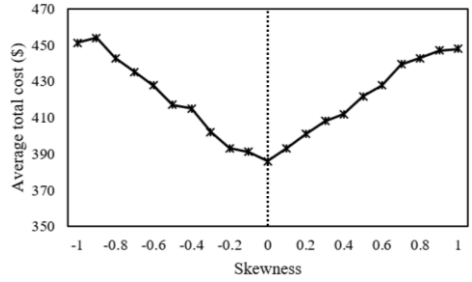

Fig. 8. Impact of distribution skewness on optimization results.

C. Considering Skewness for M-Ambiguity Set

To date, there is rare work incorporating higher moment information in ambiguity sets due to mathematical difficulty, which is also the reason that modes are regarded as fixed in this proposed M-ambiguity set. However, modes are not always located around the mean value. Therefore, a sensitivity analysis is conducted for the average total cost under various skewness. The aim is to test the impact of shiftable mode location on optimization performance. A general skewness index in the multimodal distribution is considered for all modes.

Fig. 8 shows the average total cost affected by the variation of skewness. 500 samples are used in each skewness case and 0.1 is considered as the resolution of the skewness variation. When the skewness > 0, modes generally are at the left side of the distribution and the right tail is larger. When the skewness < 0, modes generally are at the right side of the distribution and the left tail is larger. It is found that the curve is approximately symmetric around the vertical line when skewness is 0.

The result demonstrates that when skewness is 0, the average total cost is the lowest, 377.1$. However, away from 0, when the skewness is either increasing or decreasing, the cost increases because the skewness value is directly related to the forecast error distribution, thus affecting the second-stage regulation cost. The average total cost when skewness is 1 or -1 is 450$ compared with the lowest cost 377.1$, which indicates that the locations of modes are significant to optimization results, especially when the dataset is not sufficiently large.

VII. Conclusion

In this paper, a two-stage DR-EHD is proposed to accommodate the uncertainty of multimodal renewable generation to reduce system operation cost. Through extensive demonstrations, the main findings are as follows:

1. DR-EHD effectively minimizes the overall objective cost through the first-stage day-ahead preparation and real-time recourse actions at the second stage.
2. In modelling the stochastic characteristics of multimodal distribution, compared with the commonly used ambiguity set without modality information, both the multimodal and unimodal ambiguity sets are proven to be capable of mitigating the conservatism. The impact of mode location is significant proven by a sensitivity analysis of skewness.
3. Two-stage optimal scheduling plans for energy converters and ESS facilitate energy hub operators to use energy efficiently and economically to reduce operation costs.

Overall, the two-stage DR-EHD with multimodal ambiguity set guarantees the effective and efficient operation of EHS. The results from this paper justify the effectiveness and economic performance of the proposed method as compared to conventional ones, which will benefit EHS operators with less conservative scheduling plans to reduce operational costs.

In practice, the configuration of EHS remains highly similar although the specifications of energy converters, PV panels and ESS might be different. Their models can be derived by measuring their characteristics or use simplified assumptions. In addition, other uncertainties such as electricity and gas load demand can be further incorporated in the model, characterized by the proposed DRO method. In addition, other renewable resources such as wind turbines can replace PV panels, whose uncertainties can be handled by unimodal or multimodal ambiguity sets. Their data of raw output data, variance, covariance and covariance need to be obtained locally.

References

[1] M. Geidl and G. Andersson, "Optimal Power Flow of Multiple Energy Carriers," *IEEE Transactions on Power Systems*, vol. 22, pp. 145-155, 2007.
[2] W. Huang, N. Zhang, J. Yang, Y. Wang, and C. Kang, "Optimal Configuration Planning of Multi-Energy Systems Considering Distributed Renewable Energy," *IEEE Transactions on Smart Grid*, vol. 10, pp. 1452-1464, 2019.
[3] M. C. Bozchalui, S. A. Hashmi, H. Hassen, C. A. Canizares, and K. Bhattacharya, "Optimal Operation of Residential Energy Hubs in Smart Grids," *IEEE Transactions on Smart Grid*, vol. 3, pp. 1755-1766, 2012.
[4] D. Huo, C. Gu, K. Ma, W. Wei, Y. Xiang, and S. L. Blond, "Chance-Constrained Optimization for Multienergy Hub Systems in a Smart City," *IEEE Transactions on Industrial Electronics*, vol. 66, pp. 1402-1412, 2019.
[5] Y. Liang, W. Wei, and C. Wang, "A Generalized Nash Equilibrium Approach for Autonomous Energy Management of Residential Energy Hubs," *IEEE Transactions on Industrial Informatics*, pp. 1-1, 2019.
[6] T. Liu, D. Zhang, H. Dai, and T. Wu, "Intelligent Modeling and Optimization for Smart Energy Hub," *IEEE Transactions on Industrial Electronics*, pp. 1-1, 2019.
[7] B. Zhou, D. Xu, C. Li, C. Y. Chung, Y. Cao, K. W. Chan, *et al.*, "Optimal Scheduling of Biogas–Solar–Wind Renewable Portfolio for Multicarrier Energy Supplies," *IEEE Transactions on Power Systems*, vol. 33, p p. 6229-6239, 2018.

[8] S. Moazeni, A. H. Miragha, and B. Defourny, "A Risk-Averse Stochastic Dynamic Programming Approach to Energy Hub Optimal Dispatch," *IEEE Transactions on Power Systems*, vol. 34, pp. 2169-2178, 2019.
[9] M. Shahidehpour, M. Yan, X. Ai, J. Wen, N. Zhang, and C. Kang, "Robust Two-Stage Regional-District Scheduling of Multi-Carrier Energy Systems with a Large Penetration of Wind Power," *IEEE Transactions on Sustainable Energy*, pp. 1-1, 2018.
[10] M. Yan, Y. He, M. Shahidehpour, X. Ai, Z. Li, and J. Wen, "Coordinated Regional-District Operation of Integrated Energy Systems for Resilience Enhancement in Natural Disasters," *IEEE Transactions on Smart Grid*, pp. 1-1, 2018.
[11] M. Majidi and K. Zare, "Integration of Smart Energy Hubs in Distribution Networks Under Uncertainties and Demand Response Concept," *IEEE Transactions on Power Systems*, vol. 34, pp. 566-574, 2019.
[12] E. Delage and Y. Ye, "Distributionally robust optimization under moment uncertainty with application to data-driven problems," *Operations research*, vol. 58, pp. 595-612, 2010.
[13] Y. Cao, W. Wei, J. Wang, S. Mei, M. Shafie-khah, and J. P. S. Catalao, "Capacity Planning of Energy Hub in Multi-carrier Energy Networks: A Data-driven Robust Stochastic Programming Approach," *IEEE Transactions on Sustainable Energy*, pp. 1-1, 2018.
[14] P. Xiong, P. Jirutitijaroen, and C. Singh, "A Distributionally Robust Optimization Model for Unit Commitment Considering Uncertain Wind Power Generation," *IEEE Transactions on Power Systems*, vol. 32, pp. 39-49, 2017.
[15] X. Lu, K. W. Chan, S. Xia, B. Zhou, and X. Luo, "Security-Constrained Multi-Period Economic Dispatch with Renewable Energy Utilizing Distributionally Robust Optimization," *IEEE Transactions on Sustainable Energy*, pp. 1-1, 2018.
[16] P. Zhao, H. Wu, C. Gu, and I. Hernando-Gil, "Optimal home energy management under hybrid photovoltaic-storage uncertainty: a distributionally robust chance-constrained approach," *IET Renewable Power Generation*, vol. 13, pp. 1911-1919, 2019.
[17] H. Zhang, Z. Hu, E. Munsing, S. J. Moura, and Y. Song, "Data-Driven Chance-Constrained Regulation Capacity Offering for Distributed Energy Resources," *IEEE Transactions on Smart Grid*, vol. 10, pp. 2713-2725, 2019.
[18] J. Zhang, B.-M. Hodge, and A. Florita, *Investigating the Correlation Between Wind and Solar Power Forecast Errors in the Western Interconnection*, 2013.
[19] G. A. Hanasusanto, D. Kuhn, S. W. Wallace, and S. Zymler, "Distributionally robust multi-item newsvendor problems with multimodal demand distributions," *Mathematical Programming*, vol. 152, pp. 1-32, 2015.
[20] Y. Zhang, J. Le, F. Zheng, Y. Zhang, and K. Liu, "Two-stage distributionally robust coordinated scheduling for gas-electricity integrated energy system considering wind power uncertainty and reserve capacity configuration," *Renewable Energy*, vol. 135, pp. 122-135, 2019/05/01/ 2019.
[21] W. Wei, F. Liu, and S. Mei, "Distributionally Robust Co-O ptimization of Energy and Reserve Dispatch," *IEEE Transactions on Sustainable Energy*, vol. 7, pp. 289-300, 2016.
[22] Y. Ghiassi-Farrokhfal, S. Keshav, C. Rosenberg, and F. Ciucu, "Sola r Power Shaping: An Analytical Approach," *IEEE Transactions on Sustainable Energy*, vol. 6, pp. 162-170, 2015.
[23] P. Sturrock, "Analysis of bimodality in histograms formed from GALLEX and GNO solar neutrino data," *Solar Physics*, vol. 249, pp. 1-10, 2008.
[24] O. A. Jaramillo and M. A. Borja, "Wind speed analysis in La Ventosa, Mexico: a bimodal probability distribution case," *Renewable Energy*, vol. 29, pp. 1613-1630, 2004/08/01/ 2004.
[25] J. Zhang, S. Chowdhury, A. Messac, and L. Castillo, "A multivariate and multimodal wind distribution model," *Renewable Energy*, vol. 51, pp. 436-447, 2013.
[26] B. Li, R. Jiang, and J. L. Mathieu, "Ambiguous risk constraints with moment and unimodality information," *Mathematical Programming: Series A and B*, vol. 173, pp. 151-192, 2019.
[27] C. Wang, R. Gao, F. Qiu, J. Wang, and L. Xin, "Risk-Based Distributionally Robust Optimal Power Flow With Dynamic Line Rating," *IEEE Transactions on Power Systems*, vol. 33, pp. 6074-6086, 2018.
[28] F. He, "Distributionally Robust Performance Analysis: Data, Dependence and Extremes," Columbia University, 2018.
[29] D. Bertsimas, X. V. Doan, K. Natarajan, and C.-P. Teo, "Models for minimax stochastic linear optimization problems with risk aversion," *Mathematics of Operations Research*, vol. 35, pp. 580-602, 2010.
[30] J. Goh and M. Sim, "Distributionally robust optimization and its tractable approximations," *Operations research*, vol. 58, pp. 902-917, 2010.
[31] D. Bertsimas and I. Popescu, "Optimal inequalities in probability theory: A convex optimization approach," *SIAM Journal on Optimization*, vol. 15, pp. 780-804, 2005.
[32] Y. Chen, W. Wei, F. Liu, and S. Mei, "Distributionally robust hydro-thermal-wind economic dispatch," *Applied Energy*, vol. 173, pp. 511-519, 2016/07/01/ 2016.
[33] A. Ghasemi, M. Banejad, and M. Rahimiyan, "Integrated energy scheduling under uncertainty in a micro energy grid," *IET Generation, Transmission & Distribution*, vol. 12, pp. 2887-2896, 2018.
[34] Z. Hu and L. J. Hong, "Kullback-Leibler divergence constrained distributionally robust optimization," *Available at Optimization Online*, 2013.

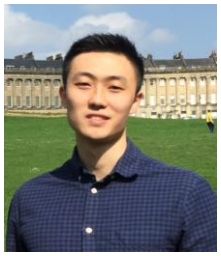

Pengfei Zhao (S'18) was born in Beijing, China. He received the double B.Eng. degree from the University of Bath, U.K., and North China Electric Power University, China, in 2017. He is currently pursuing the Ph.D. degree with the University of Bath, U.K. His research interests include the operation and planning of integrated energy systems.

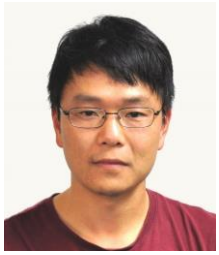

Chenghong Gu (M'14) was born in Anhui province, China. He received the Master's degree from the Shanghai Jiao Tong University, Shanghai, China, in 2007 in electrical engineering. He received the Ph.D. degree from the University of Bath, U.K. He is currently a Lecturer and EPSRC Fellow with the Department of Electronic and Electrical Engineering, University of Bath. His major research interest is in multi-vector energy system, smart grid, and power economics.

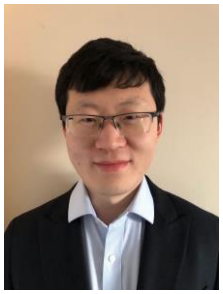

Da Huo was born in Inner Mongolia, China. He received the B.Eng. degrees in electrical and electronic engineering from the University of Bath, U.K., and in electrical power engineering from North China Electric Power University, Baoding, China, in 2014. He received the Ph.D. degree from the University of Bath, U.K, in 2018. He is currently a research associate with the School of Engineering, Newcastle University. His main research interests are multi-carrier energy system and smart grid.

Yichen Shen was born in Hebei, China. He received the double bachelor degree in electrical engineering from North China Electric Power University, China and University of Bath, U.K. in 2017. He is currently working towards the Ph.D. the University of Bath. His major research scope is resilient multi energy systems.

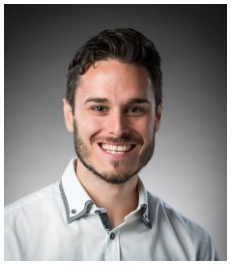

Ignacio Hernando-Gil (S'10–M'14) received the Ph.D. degree in power systems from the University of Edinburgh, U.K., in 2014. He is currently Associate Professor at ESTIA Institute of Technology, France, and was previously Prize Fellow at the University of Bath, U.K., and Research Fellow at the University of Edinburgh, U.K. He was also in industry with PassivSystems Ltd., U.K., and National Grid U.K. He has extensive research in risk modelling and analysis of active distribution networks and the aggregate impact of smart grid technologies on the quality of power supply.